nature nanotechnology

LETTERS

PUBLISHED ONLINE: 27 MARCH 2017 | DOI: 10.1038/NNANO.2017.42

Collective helicity switching of a DNA–coat assembly

Yongju Kim, Huichang Li, Ying He, Xi Chen, Xiaoteng Ma and Myongsoo Lee*

Hierarchical assemblies of biomolecular subunits can carry out versatile tasks at the cellular level with remarkable spatial and temporal precision[1,2]. As an example, the collective motion and mutual cooperation between complex protein machines mediate essential functions for life, such as replication[3], synthesis[4], degradation[5], repair[6] and transport[7]. Nucleic acid molecules are far less dynamic than proteins and need to bind to specific proteins to form hierarchical structures. The simplest example of these nucleic acid-based structures is provided by a rod-shaped tobacco mosaic virus, which consists of genetic material surrounded by coat proteins[8]. Inspired by the complexity and hierarchical assembly of viruses, a great deal of effort has been devoted to design similarly constructed artificial viruses[9,10]. However, such a wrapping approach makes nucleic acid dynamics insensitive to environmental changes. This limitation generally restricts, for example, the amplification of the conformational dynamics between the right-handed B form to the left-handed Z form of double-stranded deoxyribonucleic acid (DNA)[11,12]. Here we report a virus-like hierarchical assembly in which the native DNA and a synthetic coat undergo repeated collective helicity switching triggered by pH change under physiological conditions. We also show that this collective helicity inversion occurs during translocation of the DNA–coat assembly into intracellular compartments. Translating DNA conformational dynamics into a higher level of hierarchical dynamics may provide an approach to create DNA-based nanomachines.

The self-assembling molecules **1** and **2** consist of a bent-shaped aromatic segment with an internal angle of 120° and a hydrophilic oligoether dendron grafted at its apex, which are able to form non-covalent hexameric macrocycles with adaptable diameters to fit the size change of internal guest molecules[13]. We envisioned that the co-assembly of pyridine-based molecule **1** and pyridinium-based cationic molecule **2** might encapsulate a double-stranded DNA molecule through electrostatic interactions between pyridinium cations of the coat and negatively charged phosphate anions of DNA (Fig. 1). On adding the mixed solution of **1** and **2** (in a **1**/**2** mole ratio of 6:4) into native salmon DNA at a neutral pH (7.4), the circular dichroism (CD) spectra showed the induction of a negative Cotton effect at higher wavelengths in the spectral range of the achiral aromatic molecules (Fig. 2a and Supplementary Fig. 1). The CD signal become more apparent on increasing the content of the coat molecules up to a pyridine/phosphate (positive/negative) ratio of 1.0. (Fig. 2a and Supplementary Figs 2 and 3). This result demonstrates that binding of a DNA molecule by the pyridinium-based coat molecules induces the formation of a helical coat assembly around DNA with a preferred handedness. To visualize the formation of the DNA-induced coat assembly, we performed transmission electron microscopy (TEM) experiments on the addition of DNA (pyridine/phosphate ratio of 1:0) into the mixture of **1** and **2** at a neutral pH (7.4) (Fig. 2b). The image shows the formation of micrometre-long rod-like objects with a highly uniform diameter of ~8 nm (Supplementary Fig. 4a). With a lack of DNA, the mixture of coat molecules in a **1**/**2** mole ratio of 6:4 forms only small irregular aggregates, including short nanofibres visible when examined by TEM (Supplementary Fig. 5). This result demonstrates that the binding to DNA drives the mixture of **1** and **2** to co-assemble into a long tubular coat that surrounds a single DNA molecule. No such DNA–coat assembly was observed with pure solutions of **1** and **2**.

The dimension of the external diameter indicates that the coat assembly consists of tubular stacks of hexameric macrocycles with a single DNA molecule inside the cavity, similar to the nanoscale tubular pore reported previously[14]. Spectroscopic investigations revealed red-shifted absorption and fluorescence when compared with the molecularly dissolved state in $CHCl_3$ solution (Fig. 2c), which indicates that the aromatic segments in the coat assembly slipped with respect to each other to allow the macrocycles to be expanded to fit native DNA (2.0 nm in diameter) in the tubular cavity (Fig. 1c)[14]. This is further supported by molecular dynamics simulations, when considering the diameter of native DNA and cavity size from a slipped or overlapped packing arrangement (Supplementary Fig. 6).

Close examinations of the CD spectrum in the absorption range of DNA below 300 nm revealed a positive band at 280 nm and a negative band at 250 nm, characteristic of a right-handed B conformation (Fig. 2a)[15]. To identify further the B conformation, we performed Raman spectroscopic measurements because the scatterings in the spectral region from 600 to 700 cm^{-1} are sensitive to the conformations of DNA[16]. The Raman spectra of the DNA embedded in the coat assembly showed a characteristic band centred at 676 cm^{-1} (Fig. 3a), as expected for a canonical right-handed B conformation. This result indicates that the handedness of the DNA molecule remains unchanged even after its confinement within the coat interior at a neutral condition. To investigate the cooperative linkage between the DNA and the coat assembly in the helicity information, we performed atomic force microscopy (AFM) experiments with a DNA–coat assembly on mica in the completely dry state (Fig. 3b and Supplementary Fig. 7). The image at pH 7.4 revealed rod-like aggregates with an average diameter of 8.4 nm, consistent with that obtained from TEM. The rod-like aggregates revealed a right-handed helical structure, which demonstrates that the helicity information of the DNA transferred to the coat assembly, and thereby created a helical coat assembly with identical handedness to a canonical right-handed DNA helix.

Considering that the pK_a value of the pyridine unit in the coat molecule **1** is 5.8 (Supplementary Fig. 8), a lower pH would lead the pyridine units to be protonated, and so become more positively charged at the coat interior. Consequently, increasing the positive charge might provide a higher binding affinity to the DNA and reduce the electrostatic repulsions among the phosphate groups of DNA, which stabilize a left-handed Z conformation relative to a right-handed B form[11,12,17]. In addition, a more-efficient

State Key Laboratory of Supramolecular Structure and Materials, College of Chemistry, Jilin University, Changchun 130012, China. *e-mail: mslee@jlu.edu.cn

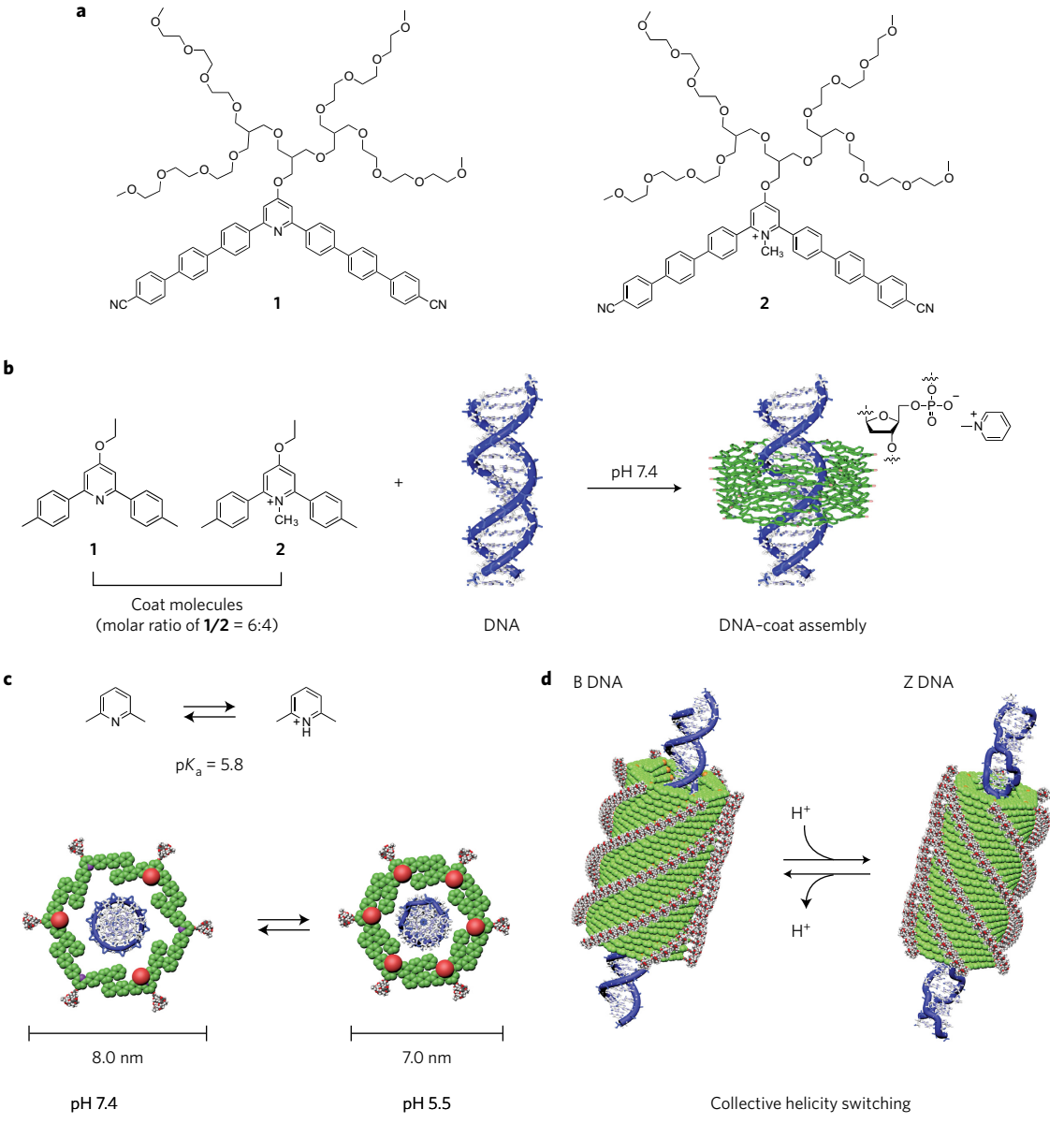

Figure 1 | Self-assembly of coat molecules driven by DNA and collective helicity switching of the DNA–coat assembly. a, Molecular structures of coat molecules **1** and **2** with pyridine and methylpyridinium, respectively. **b**, Schematic representation of the DNA–coat assembly at pH 7.4. **c**, Schematic representation of the molecular rearrangement of the coat molecules on the reversible switching of the DNA–coat assembly between expanded (pH 7.4) and contracted (pH 5.5) states. **d**, Collective motion in the helicity inversion of DNA and the synthetic coat assembly triggered by a pH change.

confinement of the DNA inside the tubular coat driven by a strengthened multivalent binding to phosphate anions would drive the relative stability of the two forms to be inverted because of the lower conformational entropy in the Z form[18,19]. Indeed, isothermal titration calorimetry (ITC) measurements revealed that the binding affinity of the coat assembly for DNA is higher at pH 5.5 ($K_a = 3.98 \times 10^4$) than at pH 7.4 ($K_a = 3.01 \times 10^4$), which indicates that the binding affinity of the coat assembly to DNA increases on lowering the pH (Supplementary Fig. 9). Raman spectra of the DNA–coat assembly at pH 5.5 showed a characteristic band associated with the Z conformation centred at 620 cm^{-1} (Fig. 3a), indicative that the DNA adopts a left-handed helical conformation[16]. This result demonstrates that the helicity of the confined DNA in the coat assembly switches from a right-handed to a left-handed helical sense triggered by a pH change. Remarkably, the helicity switching of the DNA is accompanied by helicity inversion of the coat assembly. On lowering the pH value to 5.5, the CD signal associated with the aromatic segments at longer wavelengths was inverted from the negative maximum to a strong positive Cotton effect (Fig. 3c), which indicates that the helical sense of the coat assembly switches to an opposite handedness. The AFM images at pH 5.5 revealed that the coat assembly adopts a left-handed helical conformation, which suggests that the helicity inversion of the DNA drives the coat assembly to switch simultaneously into the identical handedness through mutual interactions (Fig. 3b and Supplementary Fig. 7). This result demonstrates that the DNA–coat assembly undergoes collective motion in a helicity inversion on stimulation by a pH trigger (Fig. 1d).

To gain insight into the molecular rearrangement on changing the pH value, we carried out TEM experiments at pH 5.5 (Fig. 3d and Supplementary Fig. 4b). The image shows that the rod-like assembly structure is retained, whereas the coat size decreases from 8 to 7 nm in diameter, which indicates that the helicity inversion is accompanied by a contraction of the coat assembly

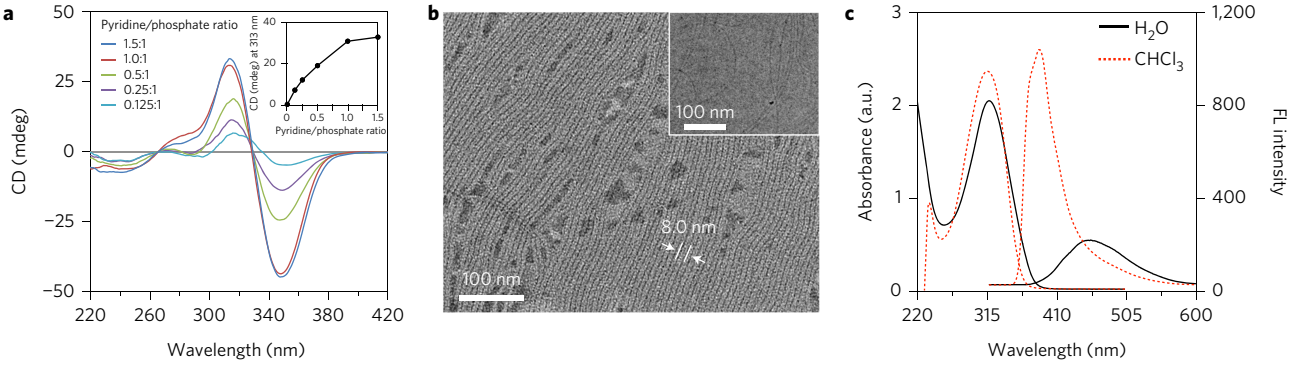

Figure 2 | Dimension and packing arrangement of the helical DNA-coat assembly at pH 7.4. a, CD spectra of the DNA-coat assembly from a series of pyridine/phosphate ratios based on the DNA solution (271 μM negatively charged phosphate) at neutral pH (7.4). The inset shows the CD intensity at 313 nm versus the pyridine/phosphate ratio. **b**, Negatively stained TEM image of the 271 μM DNA-coat assembly in pH 7.4. The inset is a cryogenic transmission electron microscopy (cryo-TEM) image. **c**, Absorption and fluorescence spectra of the 271 μM DNA-coat assembly in chloroform and a pH 7.4 buffer.

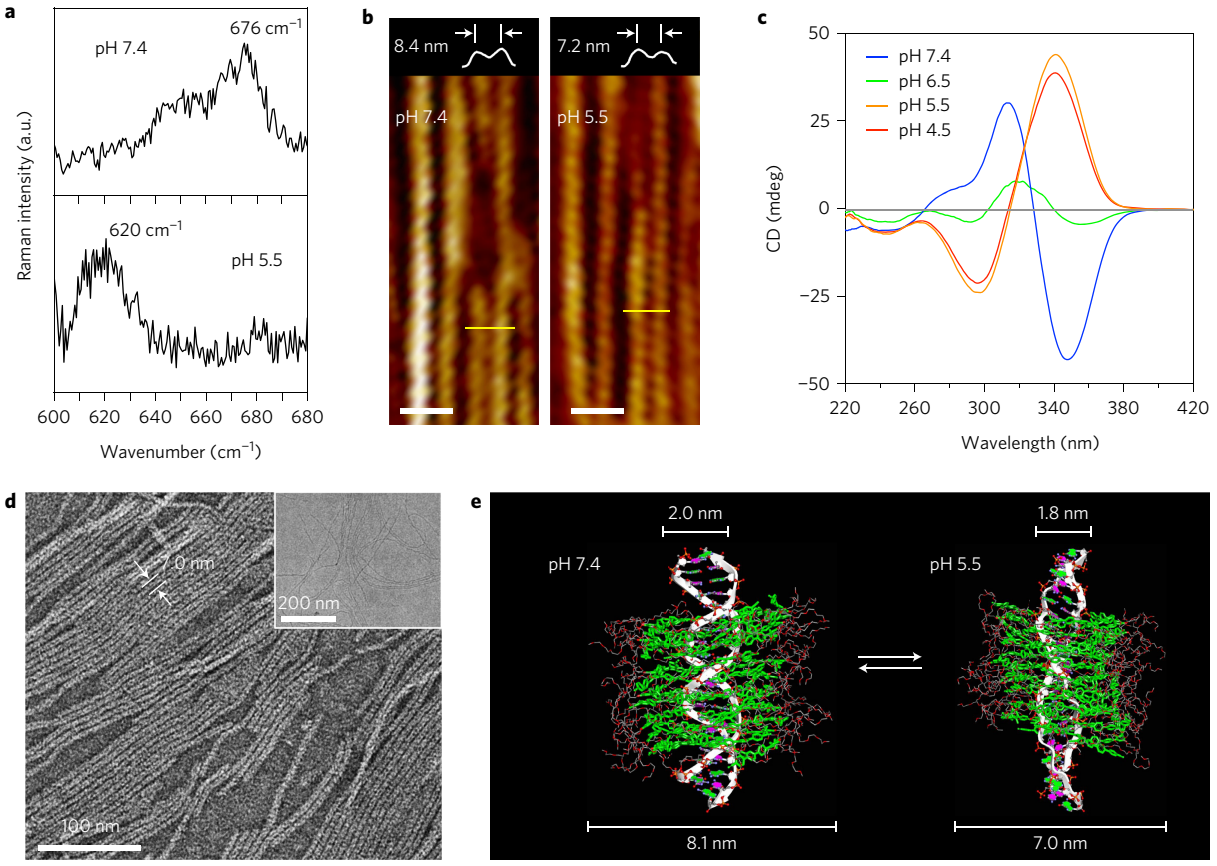

Figure 3 | Collective helicity switching triggered by a pH change. a, Raman spectra in the region from 600 to 700 cm^{-1} performed on films from the 271 μM DNA-coat assembly at pH 7.4 and pH 5.5 buffered with 5 mM potassium phosphate and sodium acetate, respectively. **b**, AFM phase images of the right-handed coat assembly (pH 7.4, left image) and left-handed coat assembly (pH 5.5, right image) on mica from films of the 271 μM DNA-coat assembly in 5 mM phosphate or acetate buffer. Scale bars, 20 nm. The cross-sectional profiles (top) are along the yellow lines. **c**, CD spectra of the 271 μM DNA-coat assembly in 5 mM buffer solutions: pH 7.4–6.5 (potassium phosphate) and pH 5.5–4.5 (sodium acetate). **d**, Negatively stained TEM image of the 271 μM DNA-coat assembly at pH 5.5 (5 mM acetate buffer). The inset is a cryo-TEM image. **e**, Molecular dynamics simulations of the expanded (pH 7.4) and the contracted (pH 5.5) states of the DNA-coat assembly. The average dimensions of the self-assembled tubular cavities with the embedded DNA were calculated to be 28.4 ± 2.6 Å and 23.4 ± 2.5 Å for B DNA and Z DNA, respectively. For clarity, the aromatic segments are visualized in green.

(Figs 1c and 3e). The contraction of the coat assembly could be attributed to a rearrangement of the aromatic segments in the coat walls that occurs with the helicity inversion of the DNA. Indeed, optical spectroscopy investigations revealed a hypochromic shift of absorption maximum and fluorescence quenching on decreasing pH (Supplementary Fig. 10), indicative of the overlapped packing arrangement of the aromatic segments[14]. At neutral conditions, the aromatic segments in the cross-section of the coat assembly are slipped with each other to fit the B-form DNA with a larger diameter (2.0 nm). On lowering the pH, however, a helicity inversion of the DNA to a Z conformation with a reduced diameter (1.8 nm) would force the coat assembly to contract through a

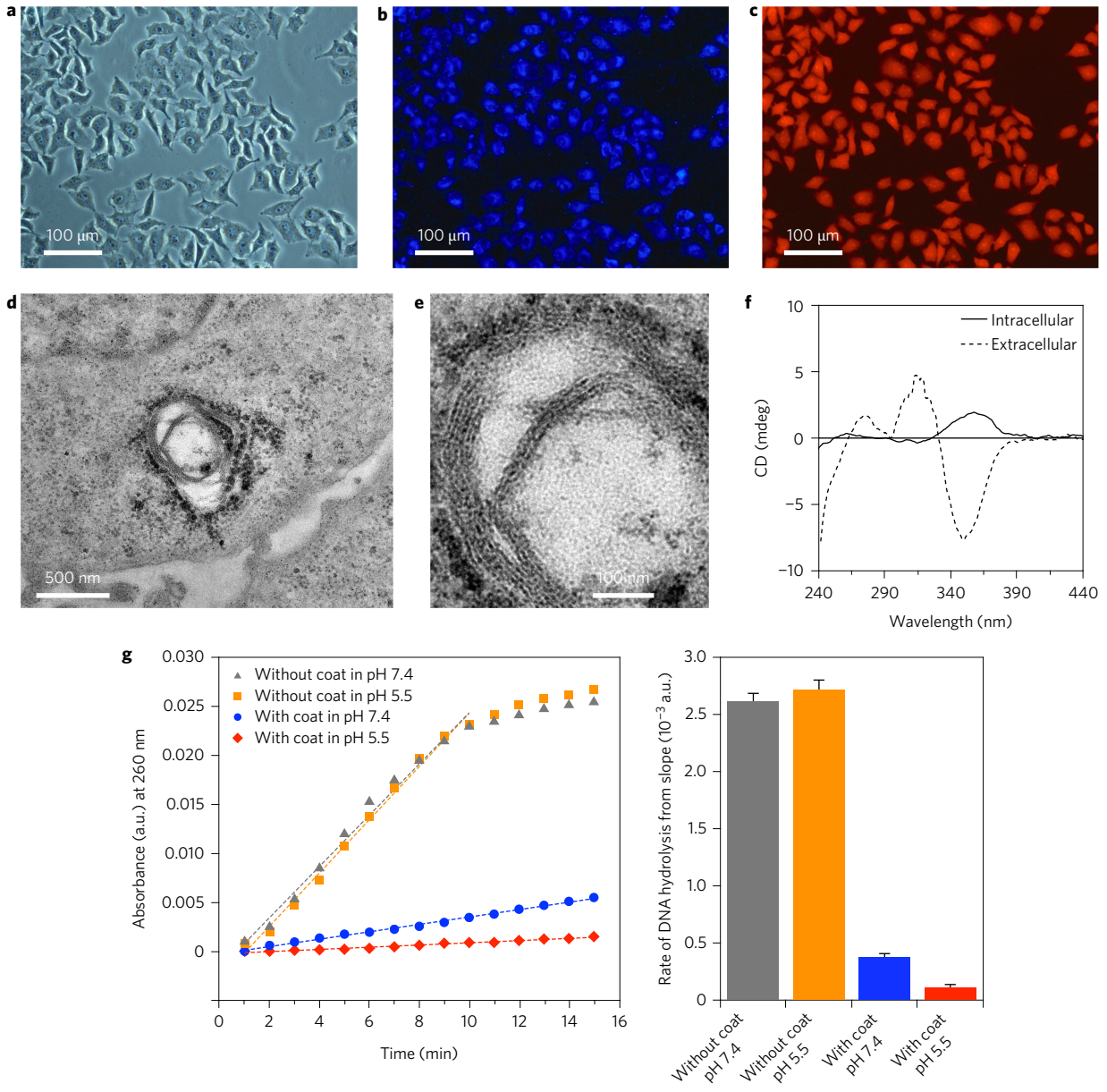

Figure 4 | Collective helicity inversion driven by translocation from the extracellular matrix to intracellular compartments. a–c, Fluorescence microscopy images after treatment of HeLa cells with the DNA–coat assembly for 24 h: bright-field (**a**), fluorescence with the excitation filter at λ_{ex} = 340–380 nm (**b**) and fluorescence with the excitation filter at λ_{ex} = 510–560 nm (**c**). **d**, TEM image of a HeLa cell with an internalized DNA–coat assembly. **e**, High-magnification micrograph of the fibre-like objects of the DNA–coat assembly inside a cell. **f**, CD spectra in the translocation of the DNA–coat assembly into intracellular compartments accompanied by helicity inversion. The CD spectra of the extracellular matrix were obtained from the DNA–coat assembly solution under reduced serum media (Opti-MEM). **g**, Rate of increase of the absorption at 260 nm by DNA on digestion with deoxyribonuclease (DNase I), depending on the existence of a coat, at different pH conditions. Data are the mean ± s.d. with n = 3 for each condition.

sliding motion between the aromatic segments to fit the DNA with a reduced size (Figs 1c and 3e). This result indicates that the coat-assembly diameter is highly flexible so that the DNA can fit, according to its helical conformations, the coat-assembly internal cavity.

The transformation of the right-handed helicity of DNA into a left-handed Z conformation can be induced by high salt concentrations or multivalent cationic polyamines, such as polylysine, polyarginine and spermines, in salt solutions through reducing the electrostatic repulsions between the phosphate anions[11,12]. In contrast, the coat assembly based on multivalent pyridinium cations induces the left-handed Z conformation even in physiological environments, which suggests that, in addition to multivalent pyridinium cations, the spatial confinement of the DNA imposed by the coat assembly induces a Z conformation. However, no such conformational change into the Z form was observed in a pure pyridine solution or pure methyl pyridinium solution irrespective of pH changes. Under acidic environments, increased concentrations of the pyridinium cations in the coat interior surface would stabilize a more compact Z conformation not only through the effect of a strengthened electrostatic screening, but also through the increased space confinement of the DNA[19]. Furthermore, the hydrophobic environment imposed by the aromatic interior of the coat assembly strengthens the electrostatic interactions, which provides additional stabilization[20,21]. Simultaneously, the strengthened interactions force the flexible-coat assembly to be contracted with helicity inversion, which leads to a collective motion of the DNA–coat assembly

(Fig. 1c,d). This is manifested in the size reduction of the coat assembly in diameter together with an enhanced binding affinity on lowering the pH (Figs 1c and 3b,d,e). The simultaneous transfer of the helicity information into the coat assembly further supports that the coat assembly is closely coupled with the DNA. Changing the pH back to 7.4 is followed by a full recovery of the coat size, which, together with the CD data, indicates that the collective motion in helicity inversion is reversible in response to a pH change (Fig. 1d). Thus, the pyridine-coated interior surface of the tubular assembly plays a key role in controlling the structural transition in which the DNA undergoes reversible switching between the two opposite helices. This allows the structural rearrangement of the coat assembly to generate a simultaneous helicity inversion through the collective interactions with the DNA.

When a non-viral vector delivers its nucleic acid cargo to a specific intracellular target, the vectors internalized by endocytosis are transported via endosomes in which the average pH is ~5 (refs 22,23). This stimulated us to envision that the lower pH values of intracellular environments would drive the DNA–coat assembly to undergo a collective helicity inversion. We thus investigated the helicity inversion of the DNA–coat assembly during the translocation into a cell by endocytosis. The translocation experiments were performed in a mammalian cell line, HeLa, a human cervical cancer cell line. Intracellular fluorescence from the cells was observed by using fluorescence microscopy after treatment of the HeLa cells with the DNA–coat assembly (Fig. 4a–c and Supplementary Fig. 11). The intracellular fluorescence distribution after the treatment of the DNA–coat assembly showed that nearly all of the cells were stained, and simultaneously showed blue (coat assembly) and red (DNA) fluorescence (Fig. 4a–c). The fluorescence microscopy images used an endosome marker to show co-localization of the DNA–coat assembly and endosomes, which indicates that the DNA–coat assembly accumulated in the endosomes during the translocation into the cell (Supplementary Fig. 12). The translocation of the DNA–coat assembly into the cells was further confirmed using TEM (Fig. 4d,e and Supplementary Fig. 13). The images of ultramicrotomed film sections revealed that the fibre-like DNA–coat assembly enters efficiently into the cells via endocytosis and accumulates in cytoplasmic compartments, most probably the endosome. In the intracellular compartment, the fibre-like structures are maintained without any noticeable structural collapse, which demonstrates that the coat assembly efficiently protects the embedded DNA against degradation under endosomal environments. The translocation of the DNA–coat assembly into the HeLa cells is accompanied by a helicity inversion because of the lower pH values inside the endosomes (Fig. 4f). The CD spectrum of the DNA–coat assembly before translocation showed a strong signal with a negative Cotton effect at 350 nm, which indicates that the right-handed helical structure is maintained in extracellular environments. On treatment with the cells, however, the CD signal was inverted from the negative minimum to a positive Cotton effect, indicative that the helical sense of the DNA–coat assembly switches to opposite handedness on translocation into the endosomes.

To explore the functional consequences of the DNA–coat assembly, we performed a kinetic study of DNA protection in a collective helicity switching of the DNA–coat assembly against enzymatic hydrolysis attack of DNase I (Fig. 4g and Supplementary Fig. 14)[24]. We found that the Z DNA inside the coat assembly showed a 3.3 times slower hydrolysis rate than the B DNA inside the coat assembly, indicative of the enhanced protection capability against enzymatic attack after the helicity transition of the DNA–coat assembly into a left-handed conformation. The enhanced protection of Z DNA against enzymatic hydrolysis could be attributed not only to a limited attack by the enzyme because of the more closely packed coat assembly at the lower pH, but also to a limited recognition of the enzyme for the left-handed Z DNA.

We have demonstrated that achiral, pyridine-based coat molecules are able to wrap native DNA to form filamentous virus-like nanostructures with simultaneous helicity switching of the DNA and its coat assembly. At pH 7.4, the embedded DNA triggers the coat assembly to induce a right-handed helical conformation, identical to that of the DNA. On lowering the pH value to 5.5, however, both the DNA and coat assembly undergo a simultaneous helicity inversion from a right- to left-handed helical sense, followed by a contraction in the diameter of the coat assembly. The collective motion in helicity switching of the DNA–coat assembly is also driven by the low pH inside endosomes during translocation into a cell. This observation also adds some insights into the puzzling biological role of the higher-energy conformer Z DNA[25].

Methods

Methods and any associated references are available in the online version of the paper.

Received 22 June 2016; accepted 17 February 2017;
published online 27 March 2017; corrected online 11 April 2017

References

1. Kinbara, K. & Aida, T. Toward intelligent molecular machines: directed motions of biological and artificial molecules and assemblies. *Chem. Rev.* **105,** 1377–1400 (2005).
2. Ishii, D. *et al.* Chaperonin-mediated stabilization and ATP-triggered release of semiconductor nanoparticles. *Nature* **423,** 628–632 (2003).
3. Sun, J. *et al.* Cdc6-induced conformational changes in ORC bound to origin DNA revealed by cryo-electron microscopy. *Structure* **20,** 534–544 (2012).
4. Alberts, B. *et al.* The cell as a collection of protein machines: preparing the next generation of molecular biologists. *Cell* **92,** 291–294 (1998).
5. Olivares, A. O. *et al.* Mechanochemical basis of protein degradation by a double-ring $A^+A^+A^+$ machine. *Nat. Struct. Mol. Biol.* **21,** 871–875 (2014).
6. Saibil, H. *et al.* Chaperone machines for protein folding, unfolding and disaggregation. *Nat. Rev. Mol. Cell Biol.* **14,** 630–642 (2013).
7. Ryan, K. J. *et al.* The nuclear pore complex: a protein machine bridging the nucleus and cytoplasm. *Curr. Opin. Cell Biol.* **12,** 361–371 (2000).
8. Butler, P. J. G. *et al.* Self-assembly of tobacco mosaic virus: the role of an intermediate aggregate in generating both specificity and speed. *Phil. Trans. R. Soc. Lond.* **354,** 537–550 (1999).
9. Lim, Y.-B. *et al.* Filamentous artificial virus from a self-assembled discrete nanoribbon. *Angew. Chem. Int. Ed.* **47,** 4525–4528 (2008).
10. Hernandez-Garcia, A. *et al.* Design and self-assembly of simple coat proteins for artificial viruses. *Nat. Nanotech.* **9,** 698–702 (2014).
11. Fuertes, M. A. *et al.* Molecular mechanisms for the B-Z transition in the example of poly[d(G-C).d((G-C)) polymers. A critical review. *Chem. Rev.* **106,** 2045–2064 (2006).
12. Choi, J. *et al.* Conformational changes of non-B DNA. *Chem. Soc. Rev.* **40,** 5893–5909 (2011).
13. Kim, H.-J. *et al.* Self-dissociating tubules from helical stacking of noncovalent macrocycles. *Angew. Chem. Int. Ed.* **139,** 8471–8475 (2010).
14. Huang, Z. *et al.* Pulsating tubules from noncovalent macrocycles. *Science* **337,** 1521–1526, (2012).
15. Kypr, J. *et al.* Circular dichroism and conformational polymorphism of DNA. *Nucl. Acids Res.* **37,** 1713–1725 (2009).
16. Benevides, J. M. *et al.* Characterization of DNA structures by Raman spectroscopy: high-salt and low-salt forms of double helical poly(dG-dC) in H_2O and D_2O solutions and application to B, Z and A-DNA. *Nucl. Acids Res.* **11,** 5747–5761 (1983).
17. Misra, V. K. *et al.* The electrostatic contribution to the B-to-Z transition of DNA. *Biochemistry* **35,** 1115–1124 (1996).
18. Sugiyama, H. *et al.* Synthesis, structure and thermodynamic properties of 8-methylguanine-containing oligonucleotides: Z-DNA under physiological salt conditions. *Nucleic Acids Res.* **24,** 1272–1278 (1996).
19. Barone, G. *et al.* Confinement effects on the interaction of native DNA with Cu(II)-5-(triethylammoniunethyl) salicylidene *ortho*-pheylendiiminate in $C_{12}E_4$ liquid crystals. *Dalton Trans.* 4172–4178 (2008).
20. Callahan, L. *et al.* B- to Z-DNA transition probed by oligonucleotides containing methylphosphonates. *Proc. Natl Acad. Sci. USA* **83,** 1617–1621 (1986).
21. Zacharias, W. *et al.* Conditions which cause the right-handed to left-handed DNA conformational transitions. *J. Biol. Chem.* **257,** 2775–2782 (1982).
22. El-Sayed, A. & Harashima, H. Endocytosis of gene delivery vectors: from clathrin-dependent to lipid raft-mediated endocytosis. *Mol. Ther.* **21,** 1118–1130 (2013).
23. Geisow, M. J. & Evans, W. H. pH in the endosome. Measurements during pinocytosis and receptor-mediated endocytosis. *Exp. Cell Res.* **150,** 36–46 (1984).

24. Kunitz, M. Crystalline desoxyribonuclease; isolation and general properties; spectrophotometric method for the measurement of desoxyribonuclease activity. *J. Gen. Physiol.* **33,** 349–362 (1950).
25. Herbert, A. & Rich, A. Left-handed Z-DNA: structure and function. *Genetica* **106,** 37–47 (1999).

Acknowledgements

This work was supported by the 1000 Program, and the National Natural Science Foundation China (no. 51473062, no. 21574055, no. 21634005 and no. 21550110493).

Author contributions

Y.K. designed and performed most of the experiments, H.L. synthesized molecules and carried out AFM experiments, Y.H. performed TEM experiments, X.C. carried out ITC experiments, X.M. performed cell cultures and imaging experiments and M.L. developed the concept, supervised the research and wrote the manuscript with input from all the authors.

Additional information

Supplementary information is available in the online version of the paper. Reprints and permissions information is available online at www.nature.com/reprints. Publisher's note: Springer Nature remains neutral with regard to jurisdictional claims in published maps and institutional affiliations. Correspondence and requests for materials should be addressed to M.L.

Competing financial interests

The authors declare no competing financial interests.

Methods

General. The morphology of the DNA–coat assembly was characterized by TEM and AFM according to the procedures reported previously[26]. Organic reagents and solvents were purchased from commercial vendors and used without further purification unless otherwise stated. DNA sodium salt from salmon testes was purchased from Sigma-Aldrich. Analytic and preparatory HPLC was performed with Prominence LC-20AP (Shimadzu) and a C18 reverse-phase column (Shim-pack Prep-ODS(H)KIT). Matrix-assisted laser desorption/ionization–time of flight spectroscopy was performed on a Bruker Autoflex TOF/TOF using α-cyano-4-hydroxy cinnamic acid as a matrix. Ultraviolet–visible spectra were obtained from a Hitachi U-2900 spectrophotometer. The fluorescence spectra were obtained from a Hitachi F-7000 fluorescence spectrophotometer. CD spectra were obtained using a Jasco J-810 spectropolarimeter.

TEM experiments. To investigate the structures of self-assembled structures in aqueous solution, a drop of an aqueous solution of the DNA–coat assembly was placed on a carbon-coated copper grid (Carbon Type B (15–25 nm) on 200 mesh) with Formvar (Ted Pella) and the solution was allowed to evaporate under ambient conditions[26]. These samples were stained by depositing a drop of uranyl acetate aqueous solution (0.2–1.0 wt%) onto the surface of the sample-loaded grid. The dried specimen was observed by using a JEOL-JEM HR2100 instrument operating at 120 kV. The cryogenic transmission electron microscopy experiments were performed with a thin film of an aqueous solution of the DNA–coat assembly (5 μl) transferred to a locally supported grid at room temperature (Lacey Formvar/Carbon, 200 mesh, Cu (Ted Pella)). The thin aqueous films were prepared under controlled temperature and humidity conditions (97–99%) within a custom-built environmental chamber to prevent evaporation of water from the sample solution. The excess liquid was blotted with filter paper for 2–3 s, and the thin aqueous films were vitrified rapidly by plunging them into liquid ethane (cooled by liquid nitrogen) at its freezing point. The grid was transferred, on a Gatan 626 cryoholder, using a cryo transfer device and transferred to a JEM HR2100 TEM. Direct imaging was carried out at a temperature of approximately −175 °C and with a 120 kV accelerating voltage, and the images were acquired with a Dual vision 300 W and SC 1000 charge-coupled device camera (Gatan). The data were analysed using Digital Micrograph software.

Raman spectroscopy experiments. The sample films on a glass slide surface were prepared by evaporation of aqueous sample solutions. The films were subjected to laser Raman spectroscopy (Jobin Ybon, T6400) equipped with an Ar-laser (514.5 nm) in air at ambient temperatures (~25 °C).

AFM experiments. The sample films on a mica surface were prepared by evaporation of aqueous sample solutions[26]. The measurements were conducted on a MultiMode 8 AFM with a NanoScope V controller, NanoScope software and NanoScope Analysis software (Bruker AXS Corporation) in air at ambient temperatures (~25 °C) with the tapping mode. Images were acquired in the PeakForce Tapping mode.

ITC. The microcalorimetric measurements for the binding study in different pH solutions were performed on an isothermal titration calorimeter (MicroCal Auto-ITC200) from GE Healthcare. The ITC instrument was periodically calibrated using the internal electric heater. Each microcalorimetric titration experiment consisted of 35 successive injections of a constant volume (1 μl per injection) of 2.71 mM DNA solution at pH 7.4 and pH 5.5, buffered with 5 mM potassium phosphate and sodium acetate, respectively, into the microcalorimetric reaction cell, filled with the coat solution (271 μM) at pH 7.4 and pH 5.5, buffered with 5 mM potassium phosphate and sodium acetate, respectively. The control experiment was also carried out by titrating DNA at the same concentration in the buffer only. The final titration curves were obtained by subtracting the control enthalpies from the enthalpies measured in the titration experiments. Binding isotherms were obtained from the integration of raw data and fitted to a one-site model. The Origin program supplied by Auto-ITC200 was used to calculate the binding constant (K_S), binding ratios (n) and molar enthalpy change (ΔH) from the titration curve.

Molecular simulations. The slipped and overlapped packing arrangement in the self-assembled tubular cavity with DNA were simulated through the MacroModel module from Schrödinger Suites (Schrödinger K.K.) with the following parameters[26]: force field, OPLS_2005; solvent, water; cutoff, Van der Waals (8.0)/electrostatic (20.0)/hydrogen bond (4.0); minimization method, PRCG (Polak–Ribiere conjugate gradient); maximum iterations, 2,500; converge on, gradient; convergence threshold, 0.05; dynamics method, stochastic dynamics; simulation temperature, 300.0 K; time step, 1.5 fs; equilibrium time, 1.0 ps; simulation time, 5,000 ps. The average distance of two hydrogens on the opposite side in a single macrocyclic layer was monitored at intervals of 50 ps as Å unit.

Determination of pK_a of the pyridine group. The pK_a value of the pyridine group of the ligand was measured by the use of NMR chemical shifts in different pH conditions[27]. Model compound **6** was dissolved in D_2O to a 1.0 mM concentration in a series of pH conditions buffered with 5 mM phosphate or acetate. The mixture was sonicated for 30 min at room temperature and equilibrated for 1 h before data acquisition. 3-(trimethylsilyl)propionic-2,2,3,3,-d_4 acid, sodium salt, was used as a chemical shift standard.

Dual fluorescent DNA–coat assembly. 0.5 ml of DNA solution (542 μM) in deionized was mixed with 0.48 ml of 10 mM buffer solutions at pH 7.4 (phosphate) and pH 5.5 (acetate). Then, 0.02 ml of 9.13 μM Goldview (excitation (λ_{ex}) 490 nm; emission (λ_{em}) 525 nm; Viswagen Biotech) for the nucleic acid stain was added to the DNA solution in the buffer to provide a final concentration of 271 μM DNA and 0.0913 μM Goldview dye at pH 7.4 and pH 5.5 buffered with 5 mM potassium phosphate and sodium acetate, respectively. These solutions were maintained for 30 min at room temperature. Then, 1 ml of the DNA solution with Goldview dye was added to a 0.271 μmol coat-molecule film, and the mixture sample was sonicated for 20 min and stabilized for 3 h at room temperature. The DNA–coat assemblies with Goldview dye in pH 7.4 and 5.5 were subjected to CD and fluorescence measurements. The fluorescence intensity was measured with λ_{ex} = 317 nm.

Cell culture with DNA–coat assembly. HeLa cells were maintained in DMEM with 10% fetal bovine serum and 1% penicillin/streptomycin in T25 culture flasks at 37 °C and 5% CO_2. The cells were collected using trypsin–EDTA, and were then counted and resuspended in reduced serum medium (Opti-MEM). The cell suspension was mixed with a DNA–coat assembly sample solution in phosphate buffer (5 mM, pH 7.4) at a final cell concentration of 1.5×10^4 cells per ml and 271 μM in a Petri dish and maintained at 37 °C and 5% CO_2 for 24 h.

Fluorescence microscopy experiments. HeLa cells (1.0×10^4 cells per ml) in Opti-MEM were incubated with a sample of the dual fluorescent DNA–coat assembly (271 μM) at 37 °C and 5% CO_2 in the Petri dish. To show co-localization of the coated DNA and the endosomes, the HeLa cells (1.0×10^4 cells per ml) in Opti-MEM were incubated with a sample of the DNA–coat assembly (271 μM) and 3 μl of the endosome marker (CellLight Late Endosomes-GFP, BacMam 2.0). After 24 h, the cells were washed with PBS solution to remove untrapped DNA–coat assembly and subjected to a Nikon Eclipse TE2000-U inverted fluorescence microscope equipped with a DXM1200C digital camera. Then, the cells, including the DNA–coat assembly, were collected using trypsin–EDTA and resuspended in PBS solution. CD spectra of the suspended cells in the PBS solution were obtained.

TEM observation of details within the cells. Observation of the details of cellular uptake of the DNA–coat assembly was performed by standard techniques described previously[28]. After the HeLa cells had been incubated for 24 h with the DNA–coat assembly, the cells were washed with PBS solution to remove untrapped DNA–coat assembly. Then the cells were collected using trypsin–EDTA solution and were prefixed with 2.5% glutaraldehyde in 0.1 M potassium phosphate buffer (pH 7.4) for 12 h at 4 °C. After fixation, the samples were washed with 0.1 M potassium phosphate buffer (pH 7.4) three times for 15 min, post-fixed with 1% OsO_4 in 0.1 M potassium phosphate buffer (pH 7.4) for 1 h at room temperature and then rinsed with 0.1 M potassium phosphate buffer (pH 7.4) three times for 15 min. The cells were dehydrated twice for 10 min in a sequence of 50, 75, 90 and 95% ethanol solutions and twice for 10 min in 100% ethanol. For embedding, samples were incubated twice for 10 min in propylene oxide, transferred to a 1:1 mixture of propylene oxide and Epon embedding resin (Epon resin (Pelco) 314 mg, DDSA (dodecenylsuccinic anhydride) 93 mg, NMA (methyl nadic anhydride) 205 mg and DMP-30 (tris(dimethylaminomethyl)phenol) 8 mg) and left in open vials for 12 h. Samples were then transferred into pure Epon embedding resin and kept in a 60 °C oven for 24 h. The block of samples was cut into thin sections (~60 nm) using a diamond knife (Diatome) on the Leica Ultracut ultramicrotome. The thin sections were transferred onto the TEM grids (3–4 sections on one grid) and stained sequentially with 1% uranyl acetate and 1% lead citrate for 3 min. The TEM grids with thin sections were washed with deionized water for 1 min and left to dry completely at room temperature. Finally, the samples were examined with a JEOL HR2100 electron microscope at 120 kV.

Measurement of deoxyribonuclease activity. The activity of the enzyme on DNA could be measured by the increase in the absorption of ultraviolet light by the digested acids[24]. DNA solution (0.5 ml, 542 μM) with or without coat molecules in 10 mM phosphate (pH 7.4) and acetate (pH 5.5) buffer were prepared. Then, 0.5 ml of 5.0 mM $MgCl_2$ and 1.0 mM $CaCl_2$ in deionized water was added to the DNA solution with or without coat molecules to provide a final concentration of 271 μM DNA and 2.5 mM $MgCl_2$ or 0.5 mM $CaCl_2$ at pH 7.4 or pH 5.5 buffered with 5 mM potassium phosphate or acetate, respectively. These solutions were maintained for 15 min at room temperature. Then, 0.2 ml of the sample solutions were added to the reference cell cuvette and the sample cell cuvette, and autozero at 260 nm was performed to provide a baseline. DNase I (RNase free, Thermo Scientific) was added to the sample-cell cuvette (3 μl for the pH 7.4 sample or 10 μl for the pH 5.5 sample). The absorbance at 260 nm was recorded at intervals of 1 min and the increase was monitored. Then, the rate of enzymatic DNA hydrolysis was expressed in terms of the slope of the plotted curve of optical density at 260 nm versus time in minutes.

The experiments were repeated three times independently. Data are presented as the mean ± s.d. Aliquots of 10 µl were taken at different times and mixed with 10 µl of 50 mM EDTA. Then, the coat molecules were removed in aliquots by extraction with ethyl acetate. After the addition of loading buffer (six times), each 20 µl sample was subjected to electrophoresis in agarose gel 1.5% at 120 V for 45 min. DNA bands were visualized using ethidium bromide under a 300 nm ultraviolet lamp.

Data availability. The data that support the findings of this study are available from the corresponding author on reasonable request.

References

26. Kim, Y. *et al.* Open–closed switching of synthetic tubular pores. *Nat. Commun.* **6,** 8650 (2015).
27. Gift, A. D., Stewart, S. M. & Bokashanga, P. K. Experimental determination of pK_a values by use of NMR chemical shifts, revisited. *J. Chem. Educ.* **89,** 1458–1460 (2012).
28. Beniash, E. *et al.* Self-assembling peptide amphiphile nanofiber matrices for cell entrapment. *Acta Biomater.* **1,** 387–397 (2005).